Electronic Supplementary Information

2D MoS_2/Polyaniline Heterostructures with Enlarged Interlayer Spacing for Superior Lithium and Sodium Storage

Haiyan Wang,[a] Hao Jiang,[a]* Yanjie Hu,[a] Neng Li,[b]* Xiujian Zhao,[b] Chunzhong Li[a]*

[a] Key Laboratory for Ultrafine Materials of Ministry of Education, School of Materials Science and Engineering, East China University of Science and Technology, Shanghai 200237, China

[b] State Key Laboratory of Silicate Materials for Architectures, Wuhan University of Technology, Wuhan, 430070, China

* Corresponding author: Tel.: +86-21-64250949, Fax: +86-21-64250624

E-mail: jianghao@ecust.edu.cn (Prof. H. Jiang), lineng@whut.edu.cn (Prof. N. Li) and czli@ecust.edu.cn (Prof. C. Z. Li)

1. Figures

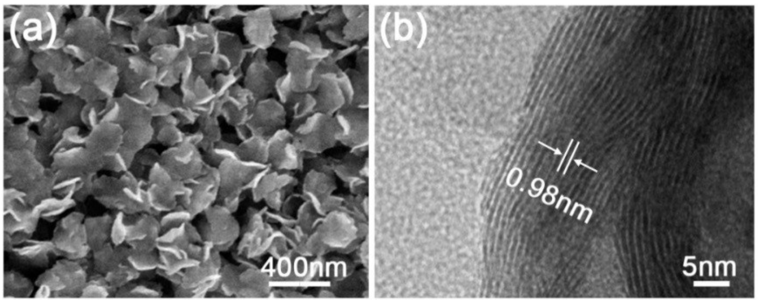

Fig. S1 (a) SEM and (b) TEM images of the MoS_2/OA nanosheets.

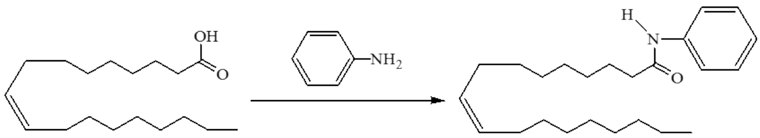

Fig. S2 The amidation reaction equation of OA and aniline.

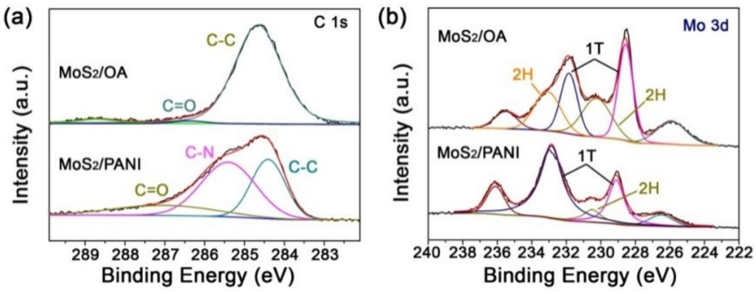

Fig. S3 XPS spectra of MoS_2/OA and MoS_2/PANI for (a) C and (b) Mo. As depicted, after the reaction with PANI, the peak corresponding to C=O at 286.4 eV shifts to 287 eV, conforming the amidation process between oleic acid and aniline. For Mo 3d spectra, the MoS_2-OA shows large double peaks at 228.6 eV ($3d_{5/2}$) and 231.8 eV ($3d_{3/2}$) and small double peaks at 230.2 eV ($3d_{5/2}$) and 233.1 eV ($3d_{3/2}$) as an evidence for the formation of MoS_2 consisting of the 1T and 2H phases. As for MoS_2/PANI, the peaks indicate an increasing of 1T phase and a decreasing of 2H phase of MoS_2, suggesting a nearly monolayer MoS_2 nanosheet, which is mainly benefit form the PANI layer in the MoS_2 interlayer effectivley avoiding their stacking/restacking. The peak Mo^{6+} $3d_{5/2}$ at 235.5 eV emerges because of partial oxidation during fabrication process. Moreover, both C and Mo peaks show a slight shift to high energy regions, indicating an electronic interaction between MoS_2 and PANI.

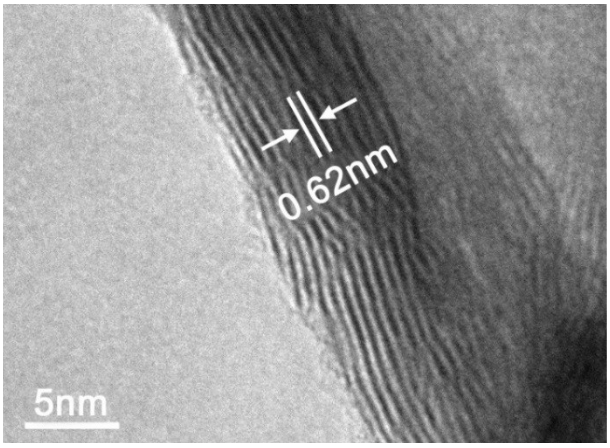

Fig. S4 TEM image of the annealed MoS_2 nanosheets.

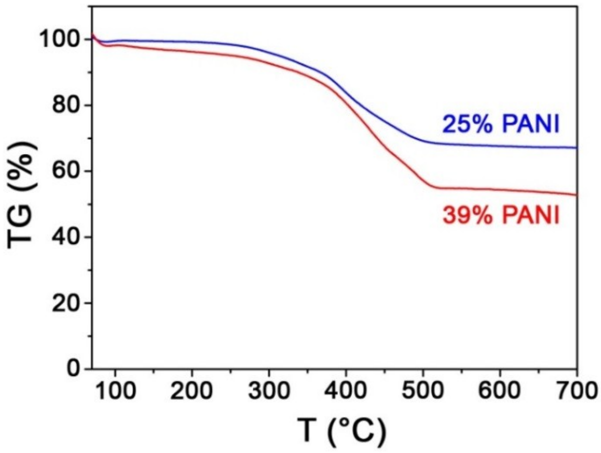

Fig. S5 TG curves of the MoS_2/PANI hybrids with different PANI content.

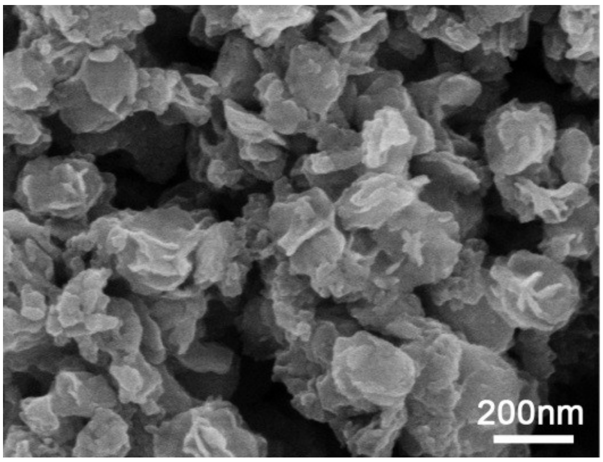

Fig. S6 SEM image of the MoS_2/PANI hybrids with 39% PANI content.

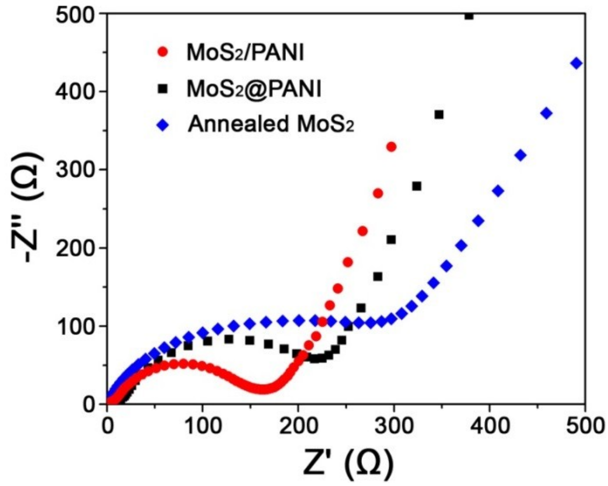

Fig. S7 Nyquist plots of the MoS_2/PANI hybrids, the MoS_2@PANI hybrids and the annealed MoS_2 nanosheets in LIBs.

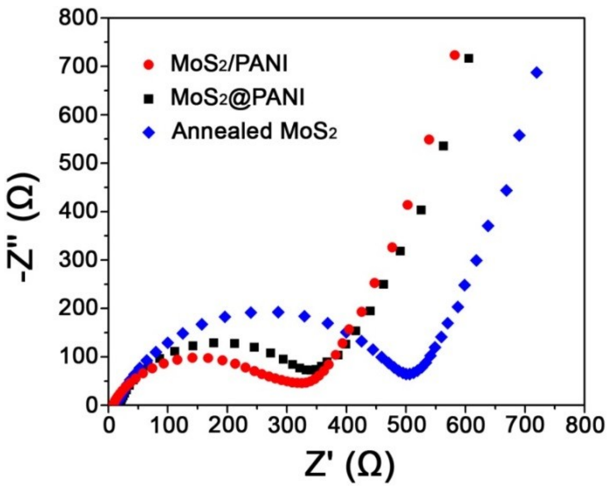

Fig. S8 Nyquist plots of the MoS_2/PANI hybrids, the MoS_2@PANI hybrids and the annealed MoS_2 nanosheets in SIBs.

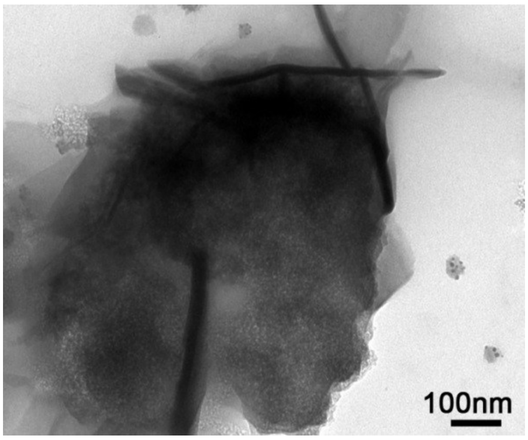

Fig. S9 TEM image of the 2D MoS_2/PANI nanosheets after 100 cycles in LIBs.

2. Tables

Table S1. Comparison of LIBs performances of MoS_2-based anode materials.

Materials	Interlayer spacing	LIBs performance	Ref.
Mesoporous MoS_2	0.66 nm	903, 845, 795 and 748 mAh g^{-1} at 100, 500, 1000 and 2000 mA g^{-1}	[1]
MoS_2 nanoplates	0.69 nm	912 mAh g^{-1} at 1062 mA g^{-1}	[1]
3D hierarchical MoS_2/polyaniline	0.64 nm	798 mA h g^{-1} at 100 mA g^{-1}, 439 mA h g^{-1} at 1000 mA g^{-1}	[3]
MoS_2/polyaniline nanowires	0.61 nm	1006 at 200 mA g^{-1}, 320 mA h g^{-1} at 1000 mA g^{-1}	[4]
MoS_2@C nanotubes	0.64 nm	1326.9, 1074.2, 993.1, and 929 mA h g^{-1} at 100, 500, 1000, and 2000 mA g^{-1}	[5]
MoS_2 nanoplates	Single-layer	1095, 986 mAh g^{-1} at 500, 1000 mA g^{-1}	[6]
3D MoS_2@Fe_3O_4 nanohybrid	Single-layer	1183, 1019 and 910 mA h g^{-1} at 100, 500 and 1000 mA g^{-1}	[7]
MoS_2@CMK-3	0.65 nm	893, 773, 713 and 591 mAh g^{-1} at 100, 500, 1000 and 2000 mA g^{-1}	[8]
3D MoS_2@porous carbon nanosheet	0.65 nm	1060, 950, 880 and 710 mA h g^{-1} at 200, 500, 1000 and 2000 mA g^{-1}	[9]
3D MoS_2 nanospheres	0.71 nm	1184.8, 882.7, 601.5, and 353.6 mAh g^{-1} at 100, 500, 1000 and 2000 mA g^{-1}	[10]
PANI/MoS_2 hybrids	1.08 nm	1319, 1285, 1247, 1152, 1077, 1029 and 885 mA h g^{-1} at 100, 200, 500, 1000, 1500, 2000 and 4000 mA g^{-1}	This work

Table S2. Comparison of SIBs performance of MoS_2-based anode materials.

Materials	Interlayer spacing	SIBs performance	Ref.
MoS_2@C nanotubes	0.64 nm	610, 560, 430 mA h g^{-1} at 50, 100 and 1000 mA g^{-1}	[5]
MoS_2 nanoplates	Singlelayer	854, 623 mA h g^{-1} at 100 and 1000 mA g^{-1}	[6]
TiO_2-B/MoS_2 nanowires	0.64 nm	214 mA h g^{-1} at 20 mA g^{-1}, 173 mA h g^{-1} at 100 mA g^{-1}, 77 mA h g^{-1} at 1000 mA g^{-1}	[11]
Exfoliated MoS_2 nanosheets	0.638 nm	500 mA h g^{-1}, 305 mA h g^{-1} at 40 mA g^{-1}, 320 mA g^{-1}	[12]
3D MoS_2–graphene microspheres	0.69 nm	427 mA h g^{-1} at 1000 mA g^{-1}	[13]
MoS_2/C nanofibers	0.64 nm	400.6 mA h g^{-1} at 50 mA g^{-1}, 369.7 mA h g^{-1} at 100 mA g^{-1}, 246.5 mA h g^{-1} at 1000 mA g^{-1}	[14]
MoS_2/C nanospheres	Not Mentioned	520 mA h g^{-1} at 67 mA g^{-1}, 390 mA h g^{-1} at 1340 mA g^{-1}	[15]
MoS_2@C paper	0.62 nm	446, 205 mA h g^{-1} at 20, 1000 mA g^{-1}	[16]
HfO_2-coated MoS_2 nanosheet	0.62 nm	613 mAh g^{-1} at 100 mA g^{-1}, 347 mAh g^{-1} at 1000 mA g^{-1}	[17]
MoS_2 nanoflowers	0.69 nm	200 mAh g^{-1} at 1000 mA g^{-1}	[18]
PANI/MoS_2 hybrids	1.08 nm	734, 634, 584, 510, 465 and 391 mA h g^{-1} at 20, 50, 100, 300, 600 and 1000 mA g^{-1}	This work

3. References

1. H. Liu, D. Su, R. Zhou, B. Sun , G. Wang, S. Qiao, *Adv. Energy Mater.,* 2012, **2**, 970–975.
2. H. Hwang, H. Kim, J. Cho, *Nano Lett.,* 2011, **11**, 4826–4830.
3. L. Hu, Y. Ren, H. Yang, Q. Xu, *ACS Appl. Mater. Interfaces,* 2014, **6**, 14644–14652.
4. L. Yang, S. Wang , J. Mao, J. Deng, Q. Gao, Y. Tang, O. G. Schmidt, *Adv. Mater.,* 2013, **25**, 1180–1184.
5. X. Zhang, X. Li, J. Liang, Y. Zhu, Y. Qian, *Small,* 2016, **12**, 2484–2491.
6. C. Zhu, X. Mu, P. A. van Aken, Y. Yu, J. Maier, *Angew. Chem. Int. Ed.,* 2014, **53**, 2152–2156.
7. X. Zhu, K. Wang, D. Yan, S. Le, R. Ma, K. Sun, Y. Liu, *Chem. Commun.,* 2015, **51**, 11888–11891.
8. X. Xu, Z. Fan, X. Yu, S. Ding, D. Yu, X. Lou, *Adv. Energy Mater.,* 2014, **4**, 1400902.
9. J. Zhou, J. Qin, X. Zhang, C. Shi, E. Liu, J. Li, N. Zhao, C. He, *ACS Nano*, 2015, **9**, 3837–3848.
10. S. Zhang, B. Chowdari, Z. Wen, J. Jin, J. Yang, *ACS Nano*, 2015, **12**, 12464–12472.
11. J. Liao, B. D. Luna, A. Manthiram, *J. Mater. Chem. A*, 2016, **4**, 801–806.
12. D. Su, S. Dou, G. Wang, *Adv. Energy Mater.,* 2014, **5**, 1401205.
13. S. H. Choi, Y. N. Ko, J. Lee, Y. C. Kang, *Adv. Funct. Mater*., 2015, **25**, 1780–1788.
14. X. Xiong, W. Luo, X. Hu, C. Chen, L. Qie, D. Hou, Y. Huang, *Sci. Rep.,* 2015, **5**, 9254.
15. J. Wang, C. Luo, T. Gao, A. Langrock, A. C. Mignerey, C. Wang, *Small,* 2015, **11**, 473–481.
16. X. Xie, T. Makaryan, M. Zhao, K. L. Van Aken, Y. Gogotsi, G. Wang, *Adv. Energy Mater.,* 2016, **6**, 1502161.
17. B. Ahmed, D. H. Anjum, M. N. Hedhili, H. N. Alshareef, *Small*, 2015, **11**, 4341–4350.
18. Z. Hu, L. Wang, K. Zhang, J. Wang, F. Cheng, Z. Tao, J. Chen, *Angew. Chem*., 2014, **126**, 13008–13012.

Movies S1-S4.